JOC The Journal of Organic Chemistry

Article

pubs.acs.org/joc

Supramolecular Recognition Induces Nonsynchronous Change of Dye Fluorescence Properties

Alba Pereira-Vilar,[†] Manuel Martin-Pastor,[‡] Marcia Pessêgo,[§] and Luis García-Río*[,†]

[†]Centro Singular de Investigación en Química Biolóxica e Materiais Moleculares (CIQUS), Departamento de Química Física, Universidade de Santiago de Compostela, 15782 Santiago de Compostela, Spain

[‡]Unidad de Resonancia Magnética (RIAIDT), Edif. CACTUS, Universidade de Santiago de Compostela, 15782 Santiago de Compostela, Spain

[§]Laboratório Associado para a Química Verde (LAQV), REQUIMTE, Departamento de Química, Faculdade de Ciências e Tecnologia, Universidade NOVA de Lisboa, 2829-516 Monte de Caparica, Portugal

Supporting Information

ABSTRACT: Fluorescence behavior of 8-anilino-1-naphthalenesulfonate (ANS) reflects a blue-shift and fluorescence enhancement on decreasing solvent polarity, with both properties affected in a synchronous way in solvent mixtures where ANS senses a homogeneous solvation shell. ANS complexation by cyclodextrins or bovine serum albumin (BSA) results in a nonhomogeneous solvation shell that is reflected by nonsynchronous variation of fluorescence properties. Steady-state fluorescence and saturation transfer difference NMR experiments allow us to conclude the formation of 1:1 and 2:1 host/guest complexes through the aniline or naphthalene moieties of ANS with cyclodextrins. This nonhomogeneous solvation shell has been ignored in studies using ANS to sense the microenvironment of proteins, micelles, bilayers, and other organized systems. ANS interaction with BSA reflects the existence of a large number of binding pockets in the surface of the protein that can be classified into two well-differentiated categories.

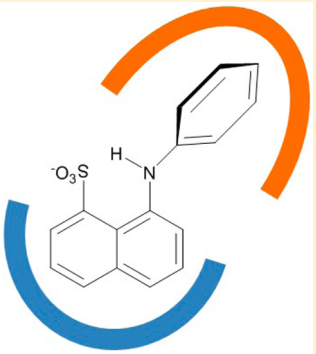

INTRODUCTION

Fluorescence dyes have attracted much attention owing to their broad use in paint, inks, textiles, and optical devices as a result of their vivid color, broad spectra, strong fluorescence intensity, and high quantum yield.[1−5] In addition, they have rather specialized applications in biodiagnostic assays. An appropriate fluorescent probe for micro-heterogeneous media (supramolecular receptors,[6−23] micelles,[24−27] vesicles,[28] microemulsions,[29,30] proteins,[31−37] etc.) shows remarkable changes in its one or more fluorescence parameters such as transition maximum, intensity, decay parameters, and anisotropy as it gets into the organized media. The sensitivity of the polarity-sensitive fluorescent molecular probe 8-anilino-1-naphthalenesulfonate (ANS) makes it a good fluorescent molecular probe for organized and aggregated systems. Additionally, compared with biological molecules, the small size of ANS enables the study around its microenvironments with little interference. The major property of this dye is that both the quantum yield as well as the maximum emission wavelength is strongly dependent on the medium polarity. An intense blue fluorescence of ANS in less polar solvents and weak green fluorescence in aqueous solutions have been observed.

The photophysical behavior of ANS in various solvents has been thoroughly studied by Kosower and co-workers.[38,39] It has been suggested that the absorption of light leads to a locally excited state $S_{1,np}$ (nonplanar (NP) geometry) that undergoes an intramolecular electron-transfer reaction to form the charge-transfer state, $S_{1,ct}$ (see Scheme 1). Plots of emission energies and quantum yields vs solvent polarity parameters show a good correlation with two different slopes. The position of the emission predominant in nonpolar solvents varies modestly with polarity and is a naphthalene-excited state, $S_{1,np}$. The great sensitivity of the second emission to solvent polarity is

Scheme 1. Excited-State Dynamics of ANS

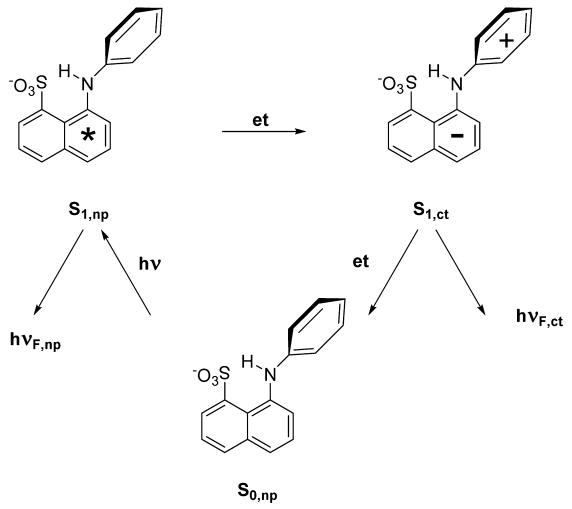

Received: May 23, 2016
Published: July 6, 2016

DOI: 10.1021/acs.joc.6b01230
J. Org. Chem. 2016, 81, 6587−6595

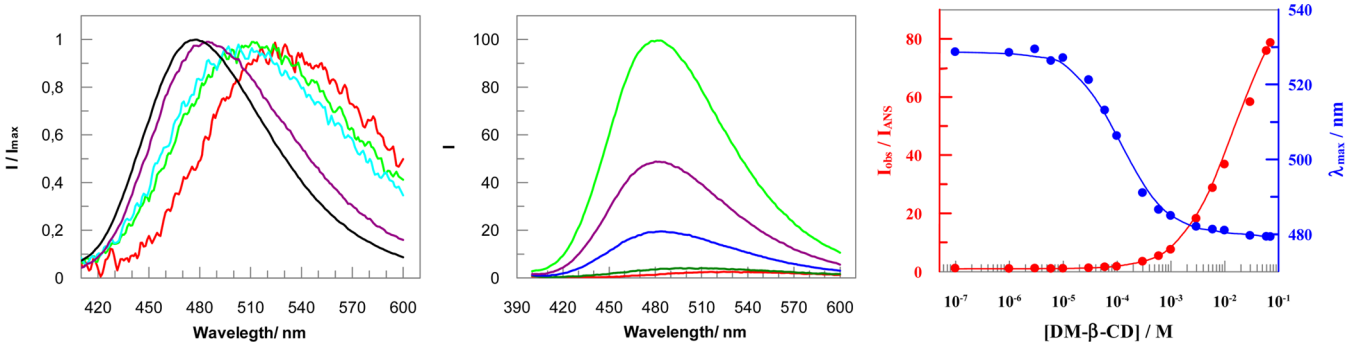

Figure 1. (Left) Normalized fluorescence spectra of 1,8-ANS (2.0×10^{-5} M) upon addition of increasing concentrations of DM-β-CD showing the blue-shift displacement of λ_{max} ([DM-β-CD] from right to left are 0; 6×10^{-5} M; 1×10^{-4} M; 1×10^{-3} M; and 7.2×10^{-3} M). (Center) Fluorescence spectra of 1,8-ANS (2.0×10^{-5} M) upon addition of increasing concentrations of DM-β-CD showing the increase in fluorescence intensity. [DM-β-CD] from bottom to top are 0; 1×10^{-4} M; 1×10^{-3} M; 3×10^{-3} M; and 1×10^{-2} M. (Right) Plot of emission maximum position (λ_{max}) and normalized fluorescence intensity (I_{obs}/I_{ANS}) at 505 nm against DM-β-CD concentration.

Scheme 2. Atom Labels for NMR Assignment

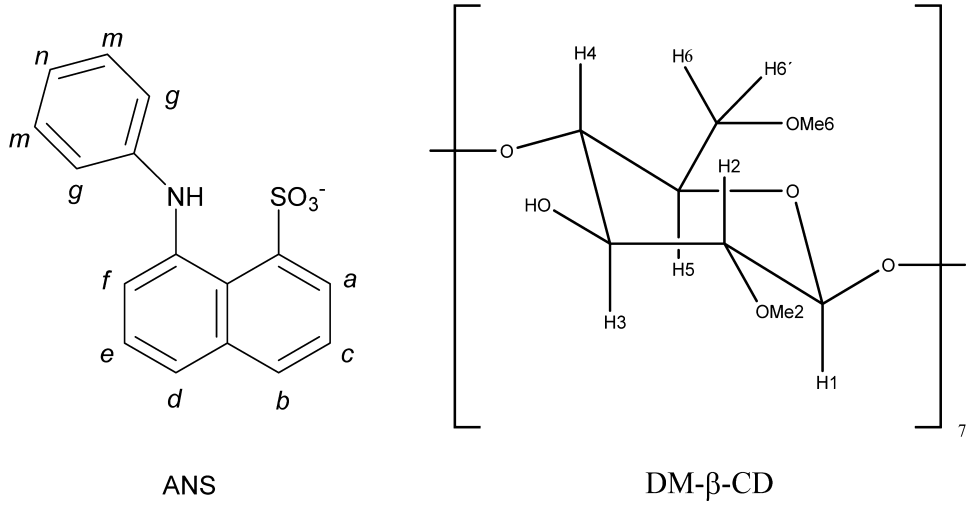

explained by a charge-transfer fluorescence from the $S_{1,ct}$ state. Moreover, it is clear that quenching of ANS fluorescence in polar solvents is a property of the $S_{1,ct}$ state. In solvent mixtures, the solvation shell around the ANS molecule is homogeneous, resulting in a synchronous variation of both wavelength of the ANS-emission maximum and the fluorescence intensity of this maximum. It is predictable than a nonhomogeneous solvation of ANS molecule will result in a nonsynchronous variation of λ_{max} and fluorescence intensity. This property is of critical relevance because ANS is widely used as a fluorescence probe to investigate properties of proteins, lipidic bilayers, gels, supramolecular, and self-assembly systems.

Here, we show clear evidence of nonsynchronous variation of fluorescence properties of ANS as a result of differential microsolvation. To this end, we investigate the incorporation of ANS to different cyclodextrin derivatives both by steady-state fluorescence and NMR. Our results show that ANS−cyclodextrin interaction is driven by inclusion of the aniline group, resulting in a change of the emission maximum forming a 1:1 host/guest complex with negligible effects on the fluorescence intensity. Further cyclodextrin addition yields a 2:1 complex where the second host interacts with the naphthalene group resulting in a large increase of fluorescence intensity. ANS bound to different receptors studied by fluorescence intensity reflects only its interaction by the naphthalene moiety, neglecting the interaction of the aniline group and so yielding a nonreal picture of the supramolecular interaction. This oversimplification is further magnified when the ANS displacement assays are carried out by competitive guests. A major goal of this work is to show that conclusions are not restricted to ANS fluorescence dye or cyclodextrins as host but are applicable to most microheterogeneous systems.

RESULTS AND DISCUSSION

Dye Incorporation in Dimethyl-β-cyclodextrin. Figure 1 shows the influence of dimethyl-β-cyclodextrin (DM-β-CD) on the fluorescence spectra of ANS ([ANS] = 2×10^{-5} M) in the presence of phosphate buffer (pH = 7.1) at 25.0 °C. As expected, the increase in fluorescence intensity with the cyclodextrin concentration parallels the blue shift displacement of λ_{max} because of the dye inclusion in the host cavity. However, a detailed analysis of the influence of [DM-β-CD] on λ_{max} and the fluorescence intensity (measured at 505 nm) shows that their variation is not synchronous. A rough estimation shows that almost 95% of the overall change in λ_{max} has been observed for [DM-β-CD] = 1×10^{-3} M; however, only 10% of the overall change in the fluorescence intensity has been reached under these experimental conditions. Asynchronous variation of λ_{max} and fluorescence intensity can be explained by considering the formation of a 1:1 host/guest complex where the aniline

DOI: 10.1021/acs.joc.6b01230
J. Org. Chem. 2016, 81, 6587−6595

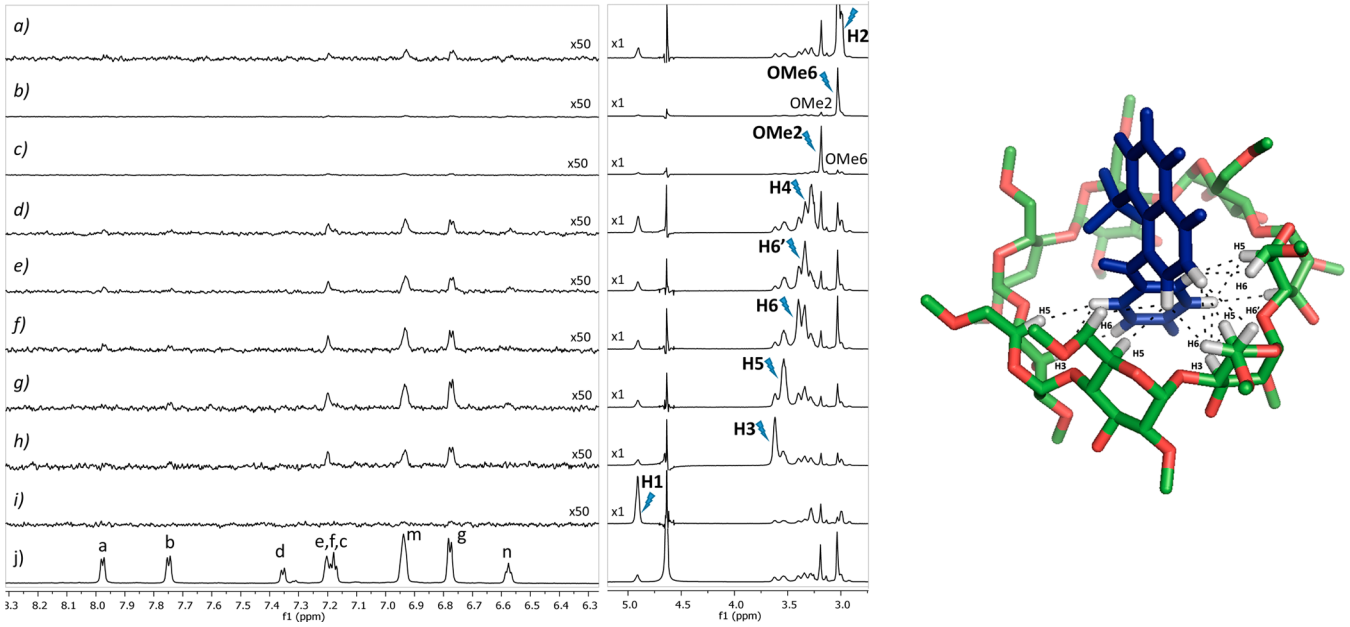

Figure 2. (Left) STD spectra obtained for the 1:1 complex. Spectra a–i are the 1D subtracted STD^{off-on} spectrum. The signal of DM-β-CD being saturated is indicated in bold and marked with an arrow. The vertical scale in the spectra of the left side is increased by a factor of 50 with respect to the corresponding spectrum on the right side. Spectrum j is the 1D STD^{off} reference spectrum. (Right) Molecular model for the DM-β-CD:ANS complex. All protons having short intermolecular STD proton–proton distances below 3.0 Å are indicated.

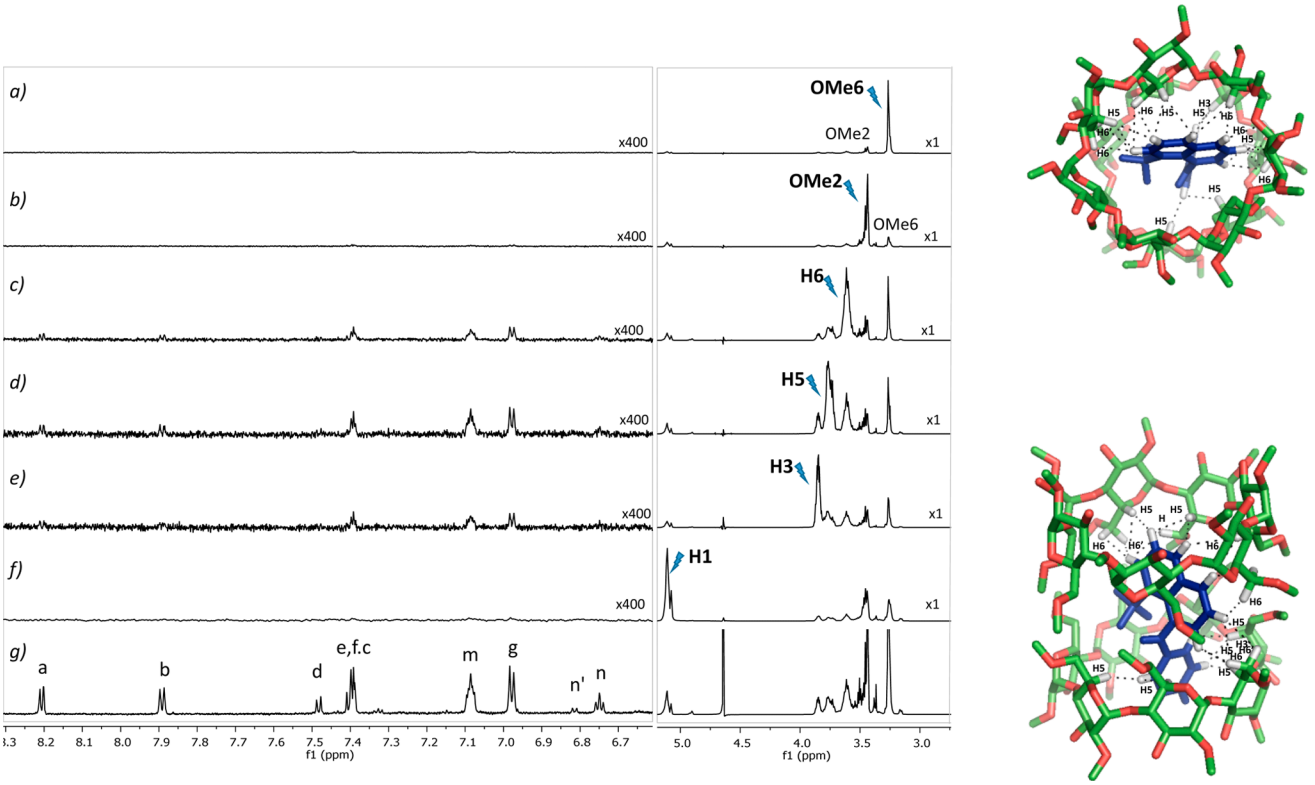

Figure 3. (Left) STD spectra obtained for the sample corresponding to the 2:1 complex. Spectra a–f are the 1D-subtracted STD^{off-on} spectra. The signal of DM-β-CD that is saturated is indicated in bold and marked with an arrow. The vertical scale in the spectra of the left side is increased by a factor of 400 with respect to the correspondingly spectrum on the right side. Spectrum g is the 1D STD^{off} reference spectrum. (Right) Molecular model of the 2:1 complex between DM-β-CD and ANS (top view and side view). All protons having short intermolecular STD proton–proton distances below 3.0 Å are indicated.

moiety is included in the DM-β-CD cavity resulting in a change in λ_{max} but mainly unaffecting the fluorescence intensity. Further increase in DM-β-CD concentration results in the formation of 2:1 complexes where the second cyclodextrin binds the naphthalene group with the subsequent fluorescence increase. Formation of 1:1 and 2:1 host/guest complexes

DOI: 10.1021/acs.joc.6b01230
J. Org. Chem. 2016, 81, 6587–6595

between β-CD and other naphthalenesulfonate derivatives has been suggested from analysis of fluorescence enhancement upon cyclodextrin complexation without further structural characterization.[40]

Further evidence concerning the structure of the 1:1 and 2:1 complexes has been obtained from NMR experiments. Samples corresponding to DM-β-CD:ANS ([DM-β-CD] = 1.0 mM; [ANS] = 0.5 mM) and DM-β-CD:ANS:DM-β-CD ([DM-β-CD] = 68 mM; [ANS] = 0.45 mM) were studied by saturation transfer difference (STD) experiments. The NMR signal assignment for the 1:1 complex was obtained by a combination of standard 2D experiments, and it is provided as Supporting Information.

Scheme 2 shows the structure of ANS and DM-β-CD molecules and the labeling convention used in the text. The STD experiment is a well-established method to determine the structure of complexes in solution. It allows a number of intermolecular proton−proton STD contacts to be made between a ligand and a receptor molecule that are interacting through a binding equilibrium.

The STD spectra obtained for the 1:1 complex are shown in Figure 2. The aromatic region of some of the STD spectra of Figure 2 shows the responses of certain peaks of the guest molecule, ANS, when some specific signals of the host, DM-β-CD, are saturated. In particular, the stronger STD peaks that are detected for the ANS molecule correspond to the protons *m*, *g*, and *n* of its phenyl ring and to protons *e* and *f* of its naphthalene ring (see Scheme 2). The mentioned STD responses appear when any of the protons H3, H5, H6, H6′, or H4 of the host molecule, DM-β-CD, are saturated (Figure 2). The saturation of protons H1, OMe2, and OMe6 of DM-β-CD essentially did not lead to STD peaks for the ANS molecule and were considered as anti-STD for the following modeling part.

A molecular mechanics optimized structure for the 1:1 complex was modeled with MM assisted by the STD results (Figure 2, right). The structure obtained is consistent qualitatively with the STD proximities and the anti-STDs observed in the spectra of Figure 2, left. The 1:1 complex essentially places the aniline ring of the ANS guest molecule at the interior of the DM-β-CD cavity where it establishes a number of STD contacts between its phenyl protons and protons H3, H5, H6, and H6′ of DM-β-CD. The naphthalene ring of ANS is relatively out of the cavity; it only establishes short intermolecular STD contacts between its protons *e* and *f* and the aforementioned protons of the host molecule. It is important to notice that in the structure of complex 1:1 protons *a* and *b* are exposed to the solvent and do not establish intermolecular STD contacts with the host molecule.

The STD spectra obtained for the DM-β-CD:ANS:DM-β-CD 2:1 complex are shown in Figure 3. The aromatic region of some STD spectra of Figure 3, left, shows a number of STD responses for certain peaks of ANS when some specific signals of the host molecule DM-β-CD are saturated, in particular, protons H3, H5, and H6. The STD responses of the guest molecule ANS in the 2:1 complex involve protons of both the phenyl and naphthalene rings (e.g., in Figure 3d the STD responses are protons *m*, *g*, *e*, *f*, *a*, and *b*). Interestingly, for the 2:1 complex there are specific STD responses of protons *a* and *b* of ANS (Figure 3c,d) that were not seen for the 1:1 complex. On the other hand, the saturation of protons H1, OMe2, and OMe6 of DM-β-CD essentially did not generate STD peaks for the ANS molecule and were considered as anti-STD for the following modeling part.

The structure of the 2:1 complex was modelized by MM calculations assisted by the STD results. There are two possibilities for modeling the 2:1 complex, one is with the two molecules of DM-β-CD disposed in a parallel arrangement and the other is with an antiparallel arrangement. In principle, the two possibilities could be distinguished by STD, as the antiparallel arrangement is the only one that permits short intermolecular STD distances between the two pendant methyl groups OMe6 and OMe2. Experimentally, the STD spectra of Figure 3a,b show the appearance of the STD peaks OMe6−OMe2 and OMe2−OMe6, respectively; they are of considerably higher intensity than in the case of the 1:1 complex (Figure 2b,c), which is in favor of the antiparallel arrangement. On the basis of these considerations, an MM-optimized structure of the 2:1 complex was obtained (Figure 3, right) that is qualitatively consistent with the intermolecular STDs and anti-STDs that are deduced from the spectra of Figure 3. Essentially, the structure of the 2:1 complex has the aniline and the naphthalene moieties of the guest molecule well inserted in the cavity of the two DM-β-CD molecules where they establish a number of intermolecular STDs with protons H3, H5, and H6. In particular, protons *a* and *b* of the naphthalene group of ANS have a number of short distances with protons H3, H5, and H6 of DM-β-CD, which is in agreement with the STD spectra of Figure 3.

Host/guest binding constants can be obtained from fluorescence experiments just considering the formation of 1:1 and 2:1 complexes (eqs 1 and 2):

$$\mathrm{CD} + \mathrm{ANS} \rightleftarrows \mathrm{CD{:}ANS} \quad K_1 = \frac{[\mathrm{CD{:}ANS}]}{[\mathrm{ANS}][\mathrm{CD}]} \tag{1}$$

$$\mathrm{CD{:}ANS} + \mathrm{CD} \rightleftarrows \mathrm{CD_2{:}ANS} \quad K_2 = \frac{[\mathrm{CD_2{:}ANS}]}{[\mathrm{CD{:}ANS}][\mathrm{CD}]} \tag{2}$$

By considering a mass balance, the following third-order equation can be obtained

$$K_1K_2[\mathrm{CD}]^3 + \{K_1 + (K_1K_2)(2[\mathrm{ANS}]_0 - [\mathrm{CD}]_0)\}[\mathrm{CD}]^2 + \{1 + K_1([\mathrm{ANS}]_0 - [\mathrm{CD}]_0)\}[\mathrm{CD}] - [\mathrm{CD}]_0 = 0 \tag{3}$$

where $[\mathrm{CD}]_0$ and $[\mathrm{ANS}]_0$ refer to the total cyclodextrin and ANS concentration and [CD] is the free cyclodextrin concentration. This equation (eq 3) has been solved for different K_1 and K_2 values, allowing us to obtain the molar fraction of free guest (X_{ANS}), 1:1 complex ($X_{\mathrm{CD:ANS}}$), and 2:1 complex ($X_{\mathrm{CD_2:ANS}}$).

Fluorescence intensity can be obtained as the molar faction weighted of the fluorescence intensity corresponding to free ANS (I_{ANS}), the 1:1 complex ($I_{\mathrm{CD:ANS}}$), and the 2:1 complex ($I_{\mathrm{CD_2:ANS}}$). Moreover, cyclodextrin concentration influence on $\lambda_{\max}$ can be obtained in a similar way, eqs 4 and 5.

$$\frac{I_{\mathrm{obs}}}{I_{\mathrm{ANS}}} = x_{\mathrm{ANS}} + \frac{I_{\mathrm{CD:ANS}}}{I_{\mathrm{ANS}}}x_{\mathrm{CD:ANS}} + \frac{I_{\mathrm{CD_2:ANS}}}{I_{\mathrm{ANS}}}x_{\mathrm{CD_2:ANS}} \tag{4}$$

$$\lambda_{\max} = \lambda_{\mathrm{ANS}}x_{\mathrm{ANS}} + \lambda_{\mathrm{CD:ANS}}x_{\mathrm{CD:ANS}} + \lambda_{\mathrm{CD_2:ANS}}x_{\mathrm{CD_2:ANS}} \tag{5}$$

DOI: 10.1021/acs.joc.6b01230
J. Org. Chem. 2016, 81, 6587−6595

Table 1. Compilation of Binding Constants, Fluorescence Increase, and λ_{max} for the 1:1 and 2:1 Complexes with Different Cyclodextrin Derivatives

	K_1 (M^{-1})	$\lambda_{CD:ANS}$ (nm)	$I_{CD:ANS}/I_{ANS}$	K_2 (M^{-1})	$\lambda_{CD_2:ANS}$ (nm)	$I_{CD_2:ANS}/I_{ANS}$
α-CD	62 ± 3	495	2.2	23 ± 3	502	8.8
β-CD	(1.2 ± 0.1) × 10^3	498	2.2	68 ± 9	501	20.2
DM-β-CD	(9.7 ± 0.1) × 10^3	481	2.1	73 ± 5	479	93.6
γ-CD	(3.7 ± 0.3) × 10^3	501	2.2	140 ± 18	496	18.0

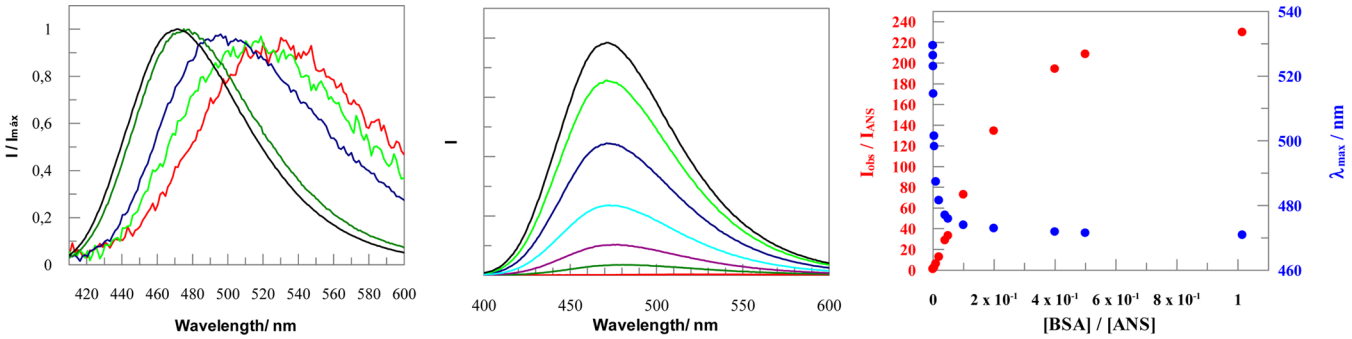

Figure 4. (Left) Normalized fluorescence spectra of 1,8-ANS (2.0×10^{-5} M) upon addition of increasing concentrations of BSA showing the blue-shift displacement of λ_{max} ([BSA] from right to left are 0; 4×10^{-8} M; 1×10^{-7} M; 1×10^{-6} M; and 2×10^{-5} M). (Center) Fluorescence spectra of 1,8-ANS (2.0×10^{-5} M) upon addition of increasing concentrations of BSA showing the increase in fluorescence intensity. [BSA] from bottom to top are 0; 4×10^{-7} M; 1×10^{-6} M; 2×10^{-6} M; 4×10^{-6} M; 8×10^{-6} M; and 2×10^{-5} M. (Right) Plot of emission maximum position (λ_{max}) and normalized fluorescence intensity (I_{obs}/I_{ANS}) at 505 nm against [BSA]/[ANS] molar ratio. [ANS] = 2.0×10^{-5} M.

A global fit of eqs 4 and 5 to the experimentally obtained fluorescence intensity and λ_{max} allow values of $K_1 = (9.7 \pm 0.1) \times 10^3$ M^{-1} and $K_2 = (73 \pm 5)$ M^{-1} (see curves in Figure 1). Table 1 compiles values for the binding constants as well as increments of fluorescence intensities for the 1:1 and 2:1 complexes and the corresponding λ_{max} values. It is well-recognized that eq 5 does not have a physical background because the wavelength of the maximum of an emission spectrum of a group of emitters is by no means additive. It could be a phenomenological tool for approximate prediction, but the correct way to determine the individual emission spectrum of each species and their fractional concentration is spectral deconvolution. Figures S-3 and S-4 in the Supporting Information show the ANS spectra deconvolution for [DM-β-CD] < 10^{-4} M as well as the molar fraction of a 1:1 complex as a function of cyclodextrin concentration. From molar fractions, a binding constant of $(9.1 \pm 0.6) \times 10^3$ M^{-1} can be obtained for the 1:1 host/guest complex. It is remarkable that binding constants obtained by spectra deconvolution and by using eq 5 are almost equal because only one binding process is observed for [DM-β-CD] < 10^{-4} M (see Figure 1). Experimental behavior observed with other cyclodextrins (see the SI) shows a clear difference between 1:1 and 1:2 complexes allowing eq 5 to be used.

As expected the increase in fluorescence intensity upon formation of the 1:1 complex is very small, just the double of the fluorescence intensity of ANS in water. Formation of the 2:1 complex upon inclusion of the naphthalene moiety results in the expected large increase in fluorescence (almost 95 times with respect to ANS in water). A similar tendency is observed for λ_{max}, as the inclusion of the aniline group in the cyclodextrin cavity is responsible for the main change in the maximum wavelength of emission.

ANS microsolvation by formation of inclusion complexes is the driving force for the asynchronous variation of fluorescence properties. This experimental behavior is not limited to DM-β-CD as was tested with similar studies carried out with other cyclodextrin derivatives, namely, α-, β-, and γ-CD (see the Supporting Information). In all cases, changes in λ_{max} are observed at low cyclodextrin concentration; meanwhile, fluorescence intensity is affected in the presence of a large host concentration as a consequence of the 2:1 complexes. The obtained binding constants and fluorescence parameters are reported in Table 1. The K_1 binding constant is smaller for α-CD than other derivatives because of the smaller size of its cavity. Larger cavity hosts show a strong binding process with DM-β-CD possessing the large K_1 value due to the large hydrophobicity of its cavity as a consequence of replacing OH by OMe groups in its structure. An analysis of the binding constants for the 2:1 complex shows that it is strongly dependent on the size of the cavity with γ-CD being the better receptor. The large size of γ-CD enables it to better accommodate the naphthalene moiety of ANS.

Fluorescence intensity is strongly compatible with the proposed model showing a very small increase on going from ANS in bulk water to the 1:1 complex independent of the size of the cyclodextrin derivative. Calculated fluorescence intensity for the 2:1 complex is affected by the size (resulting in a partial incorporation of the guest into the host, compare α- and β-CD) and hydrophobicity of the cavity. The large size of γ-CD implies that formation of inclusion complexes results in a limited release of water from its cavity in such a way that the guest is imbibed in a more hydrophilic environment than with smaller derivatives. Consequently, the naphthalene moiety is surrounded by an important number of water molecules upon its inclusion in the γ-CD resulting in a moderate increase in fluorescence. DM-β-CD shows the opposite effect, showing the larger fluorescence increase because the larger hydrophobicity of its cavity.

Values of λ_{max} are also affected by the hydrophobicity (see $\lambda_{CD:ANS}$ for DM-β-CD) and size of the cavity. Following the sequence α-, β-, and γ-CD, an increase in $\lambda_{CD:ANS}$ can be

DOI: 10.1021/acs.joc.6b01230
J. Org. Chem. 2016, 81, 6587−6595

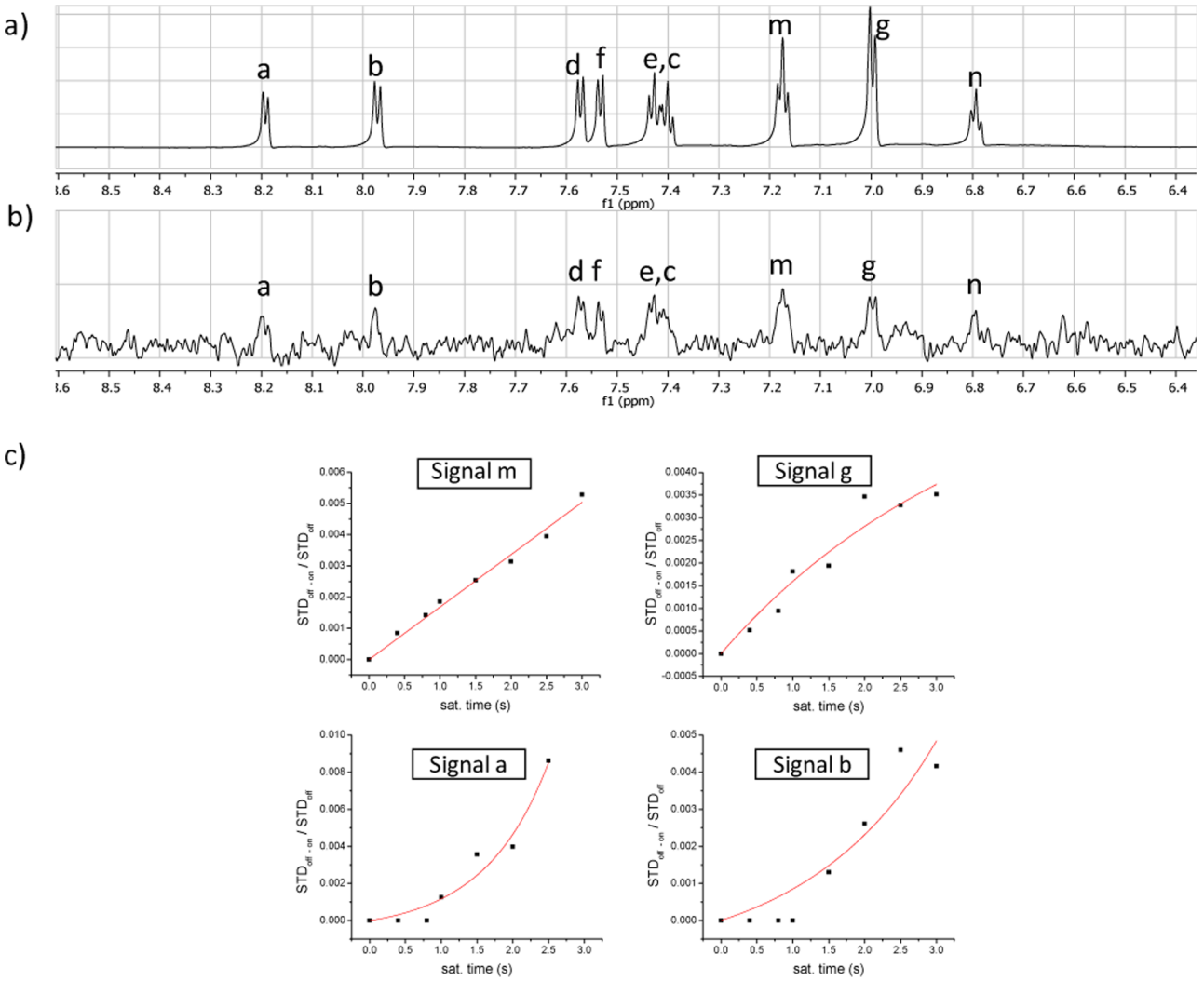

Figure 5. STD experiments of sample BSA/ANS 1:2500: (a) STD^{off} spectrum; (b) STD^{off-on} with a saturation time of 3 s; (c) STD initial build-up rate analysis of several signals of ANS to determine its correspondingly STD_0 by fitting to eqs 7 and 8.

observed on increasing the size of the receptor. The smaller cyclodextrin shows lower binding affinity for ANS, but once included into the cavity the aniline match perfectly the size of the cavity resulting in the larger effect observed for $\lambda_{CD:ANS}$. As expected for the ANS naphthalene moiety, inclusion values of $\lambda_{CD_2:ANS}$ are very close to $\lambda_{CD:ANS}$. Approach of the second cyclodextrin to form the 2:1 complex may cause a slight displacement of the anilino group outside the cavity of the first cyclodextrin resulting in an increase of $\lambda_{CD_2:ANS}$ in comparison to $\lambda_{CD:ANS}$ for α- and β-CD. The large size of γ-CD allows formation of 2:1 complexes without displacement of the guest, but increasing the hydrophobicity of the pocket yields a structure similar to that of [3]pseudorotaxane, and consequently, $\lambda_{CD_2:ANS}$ decreases in comparison to $\lambda_{CD:ANS}$.

ANS:β-CD binding processes have been widely studied in the literature[6,7,41−45] by fluorescence intensity measurements, showing values in the range 60−150 M^{-1} for the binding process simply by considering the formation of 1:1 complexes. Similarly, values of 0−5 M^{-1} have been reported[44,46] for ANS complexation by α-CD. Clearly, these studies underestimate the binding recognition process allowing wrong conclusions with strong repercussion when ANS displacement assays[10,47] are used to obtain binding constants for additional guests.

Selective Dye Complexation by Bovine Serum Albumin (BSA). The major goal of this paper is to show that nonsynchronous ANS solvation is not limited to cyclodextrins as molecular receptors. Applicability to proteins was tested by analyzing the ANS fluorescence behavior in the presence of BSA (see Figure 4) to yield a phenomenological behavior similar to that observed in the presence of cyclodextrins. An important variation in λ_{max} is observed prior to fluorescence intensity enhancement, suggesting that ANS is bound by the aniline moiety in a manner similar to that for cyclodextrins.

ANS complexation by BSA was studied by NMR under two experimental conditions: (i) a mixture of BSA:ANS was prepared at a molar ratio 1:2500 to allow a variation in fluorescence λ_{max}, keeping the quantum yield unaffected, and (ii) a molar ratio 1:100 corresponding to the experimental situation where both λ_{max} and the fluorescence intensity were affected by complexation. The STD initial build up rate methodology was applied[48,49] to determine the binding epitope of the ligand ANS in their complexes with BSA.

Parts a and b of Figure 5 show, respectively, the reference STD^{off} spectrum and the STD^{off-on} spectrum when the on-saturation was applied at 1.12 ppm, a region where the aliphatic

DOI: 10.1021/acs.joc.6b01230
J. Org. Chem. 2016, 81, 6587−6595

protons of BSA are expected and no signal of ANS is present. The appearance of signals of ANS in the later spectrum effectively demonstrate that binding occurs between ANS and BSA. To identify protons of ANS that form part of the binding epitope to BSA, a series of saturation times was explored with STD, and the intensity build-up curves of each proton of ANS are represented in Figure 5c and Figure S-8. In the plots of Figure 5c, protons *m* and *g* of ANS have a positive initial slope that identifies these protons as forming part of the binding epitope in the complexes formed with BSA. Other protons in Figure 5c and Figure S-8 have a null initial slope and therefore do not form part of the binding epitope. In these protons, the STD intensity builds up by a spin-diffusion mechanism and not by direct intermolecular proton−proton proximity with the saturated protons of the protein.[49]

Overall, the STD study carried out with the sample BSA:ANS 1:2500 proved that there is binding between ANS and BSA and that the aniline moiety of ANS forms part of the binding epitope. A similar STD study was conducted with a sample of BSA:ANS 1:100 prepared at the same concentration of ANS (see Figure S-9). In the latter case, the STD build-up plots gave positive slopes for all of the protons of ANS (see Figure S-10), indicating that at a prepared molar ratio of 1:100 there is binding between ANS and BSA and all of the protons of ANS are forming part of the binding epitope to some extent.

Experimental results indicate that BSA−ANS interaction takes place by the aniline moiety resulting in a λ_{max} blue-shift or through the naphthalene group yielding an increase in fluorescence quantum yield. It is remarkable that complexation-induced changes in fluorescence properties are not synchronous, indicating the existence of two well-differentiated binding modes. The presence of two major and structurally selective binding sites in serum albumins (sites I and II) are well-documented in the literature[50] and can explain the ANS binding modes. The binding affinity offered by site I is mainly through hydrophobic interactions, whereas site II involves a combination of hydrophobic, hydrogen bonding, and electrostatic interactions.[51,52] Despite the large body of ANS binding to serum albumins, there are large discrepancies concerning the number of binding modes and binding sites and values of binding constants. The results in Figure 4 indicate that (i) at least two ANS binding modes to BSA should be taken into consideration and (ii) the existence of a large number of binding sites in the BSA surface allows accommodation of the ANS aniline group under experimental conditions where the total ANS concentration is in large excess over protein.

CONCLUSIONS

Solvent-induced changes of fluorescence dye properties (fluorescence intensity and/or maximum emission wavelength) are well-documented in the literature, being widely used as a tool to study supramolecular, colloidal, and biological systems. Changes in composition of solvent mixtures induce solvatochromic effects with a homogeneous solvation shell around the fluorescent dye. However, probe incorporation into an organized system originates a nonhomogeneous solvation shell in such a way that different parts of the dye are sensing different microenvironments. Consequently, a nonsynchronous change in fluorescence properties is being observed as a consequence of dye incorporation into the supramolecular system. This conclusion has been tested by ANS incorporation into different cyclodextrins as is confirmed by STD NMR experiments. Experimental results indicate that aniline group incorporation into the cyclodextrin cavity induces a blue-shift of emission λ_{max}, while complexation of the naphthalene moiety forming 2:1 complexes induces an increase of fluorescence intensity. Application of nonsynchronous change in fluorescence properties must be considered as a general result, with applications in most supramolecular receptors. Biological relevance has been tested by analyzing ANS interaction with bovine serum albumin. Fluorescence and STD NMR results confirm the presence of two well-differentiated binding modes by the aniline and naphthalene moieties of the dye.

EXPERIMENTAL SECTION

8-Anilino-1-naphthalenesulfonic acid (ANS), bovine serum albumin (BSA), cyclodextrins, and deuterated water (D_2O 99% D) were commercially available. The NMR spectra were acquired on a 750 MHz spectrometer equipped with an inverse-detection triple-resonance probe $^1H/^{13}C/^{31}P$ and triple-axis-shielded PFG gradients for use with conventional 5 mm NMR tubes. The spectra were obtained at a temperature of 5 °C, and the chemical shifts reported are referenced to the lock deuterium solvent. The spectra were processed and analyzed with Mestrenova software v10.0.

For the study of the DM-*β*-CD:ANS 1:1 complex formed, an NMR sample was prepared that contained a mixture of 0.5 mM ANS and 1 mM DM-*β*-CD in D_2O. Another NMR sample was prepared for the study of the DM-*β*-CD:ANS 2:1 complex containing the mixture of 0.45 mM of ANS and 68 mM of DM-*β*-CD in D_2O.

For the study of the BSA:ANS complex, a, NMR sample was prepared as a mixture of 0.5 mM of ANS and 2×10^{-4} mM of BSA in the solvent H_2O/D_2O 90:10 v/v, resulting in a molar ratio BSA:ANS of 1:2500. Another sample was prepared with a higher proportion of BSA. It was prepared as a mixture of 0.5 mM ANS and 5×10^{-3} mM BSA in the solvents H_2O/D_2O 90:10 v/v, resulting in a molar ratio BSA:ANS 1:100. Protein solutions were prepared in 10 mM phosphate buffer (pH = 7).

NMR Experiments. The signal assignment of the ^1H and ^{13}C resonances DM-*β*-CD and ANS was obtained for the sample DM-*β*-CD:ANS 1:1 using a combination of standard 2D homo- and heteronuclear experiments. The ^1H signal assignment of the sample DM-*β*-CD:ANS 2:1 was based in the previous assignment as only modest changes in some proton chemical shifts occurred.

1D STD[48,49] experiments were acquired under similar conditions for the samples of the complexes DM-*β*-CD:ANS 1:1 and 2:1. A total of 128 scans were accumulated. In each scan, the saturation time is 3 s and the FID acquisition time is 1 s. The saturation in the on- (and off-) STD experiments consisted of a pulse train of low power selective Gaussian pulses of 50 ms separated by a 0.1 ms delay and a power of 2 dB covering a saturation bandwidth of 70 Hz. For the sample of complex DM-*β*-CD:ANS 1:1 the frequency of the train of on-saturation pulses was set, along different experiments, to each one of the following nine signals of DM-*β*-CD, where the chemical shift in ppm is given in parentheses: H_2 (3.0), OMe_6 (3.03), OMe_2(3.19), H_4 (3.28), $H_{6'}$ (3.34), H_6 (3.40), H_5 (3.54), H_3 (3.62), and H_1 (4.91). For the sample of complex DM-*β*-CD:ANS 2:1 the frequency of the train of on-saturation pulses was set to each one of the following six signals of DM-*β*-CD, along different experiments, where the number in parentheses is the value of ppm: OMe_6 (3.25), OMe_2 (3.44), H_6 (3.61), H_5 (3.76), H_3 (3.85), and H_1 (5.1). In each experiment, a similar pulse train was applied for the off-saturation but with the frequency of the pulses placed at 20 ppm. The STD_{off-on} spectrum was obtained with the scans corresponding to the STD_{on} and STD_{off} experiments interwoven during the acquisition, and the correspondingly FIDs are subtracted automatically by the phase cycling. The reference STD_{off} control spectra were also acquired by application only of the off-saturation pulse train and without any FID subtraction and half the number of scans (i.e., 64 scans).

STD[48,49] experiments were acquired for the two samples of BSA:ANS 1:2500 and BSA:ANS 1:100. The pulse sequence included a soft-watergate scheme prior to the FID acquisition to suppress the

DOI: 10.1021/acs.joc.6b01230
J. Org. Chem. 2016, 81, 6587−6595

strong water peak. The train of saturation pulses used for the on- and off-STD spectra used the same conditions that those described above for the STD experiments of the DM-β-CD:ANS samples. The soft-watergate scheme used is based on the DPFGSE (double pulse field gradient spin echo)[53] scheme and applies Gaussian selective 180 deg pulses of 2.4 ms over the water frequency (~4.7 ppm). The frequency of the saturation for the STD_{on} spectrum was placed at 1.12 ppm corresponding to the region were the aliphatic protons of BSA are expected. The saturation frequency in the STD_{off} spectrum was placed at 20 ppm. The STD_{off-on} spectrum was obtained with interleaved acquisition of STD_{off} and STD_{on} experiments and auto-subtraction of the FIDs by phase cycling. The STD spectra (on- and off-) were measured by exploring a series of saturation times and under a constant scan duration of 4 s that includes a period of 1 s for the FID acquisition time. For sample BSA:ANS 1:2500, each STD was measured with 2300 scans, and the saturation times explored (t_{sat}) were 0.4, 0.8, 1, 1.5, 2, 2.5, and 3 s. For sample BSA:ANS 1:100, each STD was measured with 640 scans, and the values of t_{sat} explored were 0.05, 0.2, 0.4, 0.6, 0.8, 1, 1.2, 1.6, 2, 2.5, and 3 s.

At a certain saturation time, the value of STD was evaluated from the corresponding signal intensity in the off- and on-spectra using eq 6.

$$\mathrm{STD} = \frac{\mathrm{STD_{off}} - \mathrm{STD_{on}}}{\mathrm{STD_{off}}} \tag{6}$$

For each sample, the binding epitope of the ANS ligand in its complex with BSA was determined with the STD initial build-up rate method.[48,49] In this method, the STD of a given signal is represented at the series of t_{sat} explored. The curve is nonlinearly fitted to eq 7 to determine STD_{max} and k_{sat}.

$$\mathrm{STD}(t_{sat}) = \mathrm{STD_{max}}[1 - e^{(-k_{sat}\cdot t_{sat})}] \tag{7}$$

The slope of the curve at zero saturation time (STD_0) determines the binding epitope; it is calculated by the following expression:

$$\mathrm{STD_0} = \mathrm{STD_{max}} k_{sat} \tag{8}$$

Molecular Modeling. Molecular mechanics (MM) calculations with the CHARMM force field were performed using software VEGA ZZ to deduce plausible structures of the complexes DM-β-CD:ANS 1:1 and 2:1. The initial structure of DM-β-CD was built based in the X-ray structure of β-cyclodextrin in which all the sugar rings adopt a stable $^4C_1$ chair conformation. The hydroxymethyl of the seven sugar residues of DM-β-CD were set in the stable gauche−gauche conformations (torsion angle $\omega = -60°$ defined by atoms $O_5-C_5-C_6-O_6$ of the sugar ring) which leaves the hydroxymethyl hydrogens H_6 and $H_{6'}$ pointing toward the interior of the cavity. The latter permits the existence of intermolecular NOEs between the two H_6 and $H_{6'}$ protons of DM-β-CD and some protons of ANS, which is consistent with the STD results. The initial structure of DM-β-CD was exhaustively optimized by MM energy minimization. The structure of the free ligand ANS was built including a sodium counterion to neutralize the charge of its sulfite group and submitted to MM energy minimization. Initial molecular models of the complexes DM-β-CD:ANS 1:1 and 2:1 were built by docking ANS in the cavity of DM-β-CD. From the different possibilities for performing the docking, the only possibility considered was the one that was qualitatively consistent with the experimental NOE contacts between protons of DM-β-CD and ANS deduced from the experimental STD responses. The modeling of the DM-β-CD:ANS 2:1 complex was performed with two possible initial structures, one with the two DM-β-CD molecules disposed in antiparallel arrangement and another one with parallel arrangement as discussed in the text. The initial models of the complexes DM-β-CD:ANS 1:1 and 2:1 were exhaustively minimized by MM and the final structures more compatible with STD data were represented with Pymol software.

Single Binding Model. The model used is based on the assumption that a 1:1 complex is formed between the DM-β-CD and the ANS.

$$\mathrm{ANS} + \text{DM-}\beta\text{-CD} \overset{K_1}{\rightleftarrows} \mathrm{CD{:}ANS} \tag{9}$$

The stability of the inclusion complex can be described as an association constant, K_1, $K_1 = \frac{[\mathrm{CD{:}ANS}]}{[\mathrm{CD}][\mathrm{ANS}]}$ where [CD] and [ANS] represent the equilibrium concentration of free species and [CD:ANS] is the concentration of the 1:1 complex. The mass balance for the total concentraions of CD and ANS are given by $[\mathrm{CD}]_0 = [\mathrm{CD}] + [\mathrm{CD{:}ANS}]$ and $[\mathrm{ANS}]_0 = [\mathrm{ANS}] + [\mathrm{CD{:}ANS}]$. The combination of these equations with the binding constant gives a second-order equation for the concentration of uncomplexed CD.

$$K_1[\mathrm{CD}]^2 + \{1 + K_1([\mathrm{ANS}]_0 - [\mathrm{CD}]_0)\}[\mathrm{CD}] - [\mathrm{CD}]_0 = 0 \tag{10}$$

This second-order equation was solved for different values of K_1 in order to obtain the [CD]. The value of K_1 for which we obtain the best root-mean-square deviation values in the fitting of the experimental results was taken as optimal.

■ ASSOCIATED CONTENT

Supporting Information

The Supporting Information is available free of charge on the ACS Publications website at DOI: 10.1021/acs.joc.6b01230.

NMR assignment of free ANS and 1:1 complex; influence of α-, β-, and γ-CD on ANS fluorescence; STD experiments of ANS in the presence of BSA; atom coordinate and energies of molecular models (PDF)

■ AUTHOR INFORMATION

Corresponding Author

*E-mail: luis.garcia@usc.es.

Notes

The authors declare no competing financial interest.

■ ACKNOWLEDGMENTS

This work was supported by the Ministerio de Economia y Competitividad of Spain (project CTQ2014-55208-P), Xunta de Galicia (GRC2007/085). and the Associated Laboratory for Sustainable Chemistry−Clean Processes and Technologies−LAQV, which is financed by national funds from FCT/MEC (UID/QUI/50006/2013) and cofinanced by the ERDF under a PT2020 Partnership Agreement (POCI-01-0145-FEDER-007265).

■ REFERENCES

(1) De Rosa, M. C.; Hodgson, D. J.; Enright, G. D.; Dawson, B.; Evans, C. E. B.; Crutchley, R. J. *J. Am. Chem. Soc.* **2004**, *126*, 7619−7626.

(2) Sadhu, V. B.; Perl, A.; Péter, M.; Rozkiewicz, D. I.; Engbers, G.; Ravoo, B. J.; Reinhoudt, D. N.; Huskens, J. *Langmuir* **2007**, *23*, 6850−6855.

(3) Lemke, E. A.; Gambin, Y.; Vandelinder, V.; Brustad, E. M.; Liu, H. W.; Schultz, P. G.; Groisman, A.; Deniz, A. A. *J. Am. Chem. Soc.* **2009**, *131*, 13610−13612.

(4) Lu, H. P.; Mai, C. L.; Tsia, C. Y.; Hsu, S. J.; Hsieh, C. P.; Chiu, C. L.; Yeh, C. Y.; Diau, E. W. G. *Phys. Chem. Chem. Phys.* **2009**, *11*, 10270−10274.

(5) Knoll, W.; Yu, F.; Neumann, T.; Schiller, S.; Naumann, R. *Phys. Chem. Chem. Phys.* **2003**, *5*, 5169−5175.

(6) Yang, J.; Xiang, J.; Chen, C.; Lu, D.; Xu, G. *J. Colloid Interface Sci.* **2001**, *240*, 425−431.

(7) Wagner, B. D.; MacDonald, P. J. *J. Photochem. Photobiol., A* **1998**, *114*, 151−157.

(8) Shi, Y.; Wang, D.; Zhang, Z. *J. Photochem. Photobiol., A* **1995**, *91*, 211−215.

(9) Lagrost, C.; Alcaraz, G.; Bergamini, J. F.; Fabre, B.; Serbanescu, I. *Chem. Commun.* **2007**, 1050−1052.

DOI: 10.1021/acs.joc.6b01230
J. Org. Chem. 2016, 81, 6587−6595

(10) Park, J. W.; Song, H. J. *J. Phys. Chem.* **1989**, *93*, 6454−6458.
(11) Bright, F. V.; Catena, G. C.; Huang, J. *J. Am. Chem. Soc.* **1990**, *112*, 1343−1346.
(12) Tabushi, I.; Sasaki, H.; Kuroda, Y. *J. Am. Chem. Soc.* **1976**, *98*, 5727−5728.
(13) Wagner, B. D.; Stojanovic, N.; Day, A. I.; Blanch, R. J. *J. Phys. Chem. B* **2003**, *107*, 10741−10746.
(14) Wagner, B. D.; MacRae, A. I. *J. Phys. Chem. B* **1999**, *103*, 10114−10119.
(15) Grandini, P.; Mancin, F.; Tecilla, P.; Scrimin, P.; Tonellato, U. *Angew. Chem., Int. Ed.* **1999**, *38*, 3061−3064.
(16) Arimura, T.; Nagasaki, T.; Shinkai, S.; Matsuda, T. *J. Org. Chem.* **1989**, *54*, 3766−3768.
(17) Wagner, B. D.; Fitzpatrick, S. J. *J. Inclusion Phenom. Mol. Recognit. Chem.* **2000**, *38*, 467−478.
(18) Liu, Y.; You, C.-C. *J. Phys. Org. Chem.* **2001**, *14*, 11−16.
(19) Dsouza, R. N.; Pischel, U.; Nau, W. N. *Chem. Rev.* **2011**, *111*, 7941−7980.
(20) Sayed, M.; Pal, H. *J. Mater. Chem. C* **2016**, *4*, 2685−2706.
(21) Yu, G.; Wu, D.; Li, Y.; Zhang, Z.; Shao, L.; Zhou, J.; Hu, Q.; Tang, G.; Huang, F. *Chem. Sci.* **2016**, *7*, 3017−3024.
(22) Yu, G.; Tang, G.; Huang, F. *J. Mater. Chem. C* **2014**, *2*, 6609−6617.
(23) Wang, P.; Yan, X.; Huang, F. *Chem. Commun.* **2014**, *50*, 5017−5019.
(24) Abuin, E. B.; Lissi, E. A.; Aspée, A.; Gonzalez, F. D.; Varas, J. M. *J. Colloid Interface Sci.* **1997**, *186*, 332−338.
(25) Kim, W.; Thévenot, J.; Ibarboure, E.; Lecommandoux, S.; Chaikof, E. L. *Angew. Chem., Int. Ed.* **2010**, *49*, 4257−4260.
(26) Abuin, E. B.; Lissi, E. A.; Borsarelli, C. *J. Colloid Interface Sci.* **1996**, *184*, 652−657.
(27) Das, D.; Dasgupta, A.; Roy, S.; Mitra, R. N.; Debnath, S.; Das, P. K. *Chem. - Eur. J.* **2006**, *12*, 5068−5074.
(28) Mohapatra, M.; Mishra, A. K. *Langmuir* **2013**, *29*, 11396−11404.
(29) Patra, A.; Luong, T. Q.; Mitra, R. K.; Havenith, M. *Phys. Chem. Chem. Phys.* **2014**, *16*, 12875−12883.
(30) Glenn, K. M.; Palepu, R. M. *J. Photochem. Photobiol., A* **2006**, *179*, 283−288.
(31) Takehara, K.; Morinaga, Y.; Nakashima, S.; Matsuoka, S.; Kamaya, H.; Ueda, I. *Anal. Sci.* **2006**, *22*, 1571−1575.
(32) Gee, M. L.; Lensun, L.; Smith, T. A.; Scholes, C. A. *Eur. Biophys. J.* **2004**, *33*, 130−139.
(33) Togashi, D. M.; Ryder, A. G. *J. Fluoresc.* **2008**, *18*, 519−526.
(34) Togashi, D. M.; Ryder, A. G.; O'Shaughnessy, D. *J. Fluoresc.* **2010**, *20*, 441−452.
(35) Tagore, R.; Thomas, H. R.; Homan, E. A.; Munawar, A.; Saghatelian, A. *J. Am. Chem. Soc.* **2008**, *130*, 14111−14113.
(36) Marianayagam, N. J.; Khan, F.; Male, L.; Jackson, S. E. *J. Am. Chem. Soc.* **2002**, *124*, 9744−9750.
(37) Banerjee, T.; Kishore, N. *J. Phys. Chem. B* **2006**, *110*, 7022−7028.
(38) Kosower, E. M.; Kanety, H. *J. Am. Chem. Soc.* **1983**, *105*, 6236−6243.
(39) Kosower, E. M.; Huppert, D. *Annu. Rev. Phys. Chem.* **1986**, *37*, 127−156.
(40) Harada, A.; Furue, M.; Nozakura, S. *Macromolecules* **1977**, *10*, 676−681.
(41) Sueishi, Y.; Fujita, T.; Nakatani, S.; Inazumi, N.; Osawa, Y. *Spectrochim. Acta, Part A* **2013**, *114*, 344−349.
(42) Hoenigman, S. M.; Evans, C. E. *Anal. Chem.* **1996**, *68*, 3274−3276.
(43) Liu, Y.; Duan, Z.-Y.; Chen, Y.; Han, J.-R.; Cui, L. *Org. Biomol. Chem.* **2004**, *2*, 2359−2364.
(44) Schneider, H. J.; Blatter, T.; Simova, S. *J. Am. Chem. Soc.* **1991**, *113*, 1996−2000.
(45) Liu, Y.; Li, X.-Q.; Chen, Y.; Guan, X.-D. *J. Phys. Chem. B* **2004**, *108*, 19541−19549.
(46) Franke, J.; Merz, F.; Lorensky, H. W.; Muller, W. M.; Werner, W.; Vagtle, F. *J. Inclusion Phenom.* **1985**, *3*, 471−478.
(47) Tabushi, I.; Kuroda, Y.; Mizutani, T. *J. Am. Chem. Soc.* **1986**, *108*, 4514−4518.
(48) Meyer, B.; Peters, T. *Angew. Chem., Int. Ed.* **2003**, *42*, 864−890.
(49) Mayer, M.; Meyer, B. *Angew. Chem., Int. Ed.* **1999**, *38*, 1784−1788.
(50) Sudlow, G.; Birkett, D. J.; Wade, D. N. *Mol. Pharmacol.* **1975**, *11*, 824−832.
(51) Jimenez, M. C.; Miranda, M. A.; Vaya, I. *J. Am. Chem. Soc.* **2005**, *127*, 10134−10135.
(52) Jisha, V. S.; Arun, K. T.; Hariharan, M.; Ramaiah, D. *J. Am. Chem. Soc.* **2006**, *128*, 6024−6025.
(53) Liu, M.; Mao, X.-A.; Ye, Ch.; Huang, H.; Nicholson, J. K.; Lindon, J. C. *J. Magn. Reson.* **1998**, *132*, 125−129.

DOI: 10.1021/acs.joc.6b01230
J. Org. Chem. 2016, 81, 6587−6595